IEEE Access
Multidisciplinary | Rapid Review | Open Access Journal

Received November 1, 2018, accepted November 30, 2018, date of publication February 1, 2019, date of current version February 12, 2019.

Digital Object Identifier 10.1109/ACCESS.2018.2889738

Assessment of Energy Management in a Fuel Cell/Battery Hybrid Vehicle

MAURO CARIGNANO[1], VICENTE RODA[2], RAMON COSTA-CASTELLÓ[2], (Senior Member, IEEE), LUIS VALIÑO[3], ANTONIO LOZANO[3], AND FÉLIX BARRERAS[3]

[1]Facultad de Ciencias Exactas Ingeniería y Agrimensura, Universidad Nacional de Rosario, CONICET, Rosario S2000, Argentina
[2]Institut de Robòtica i Informàtica Industrial, CSIC-UPC, 08028 Barcelona, Spain
[3]Laboratory for Research in Fluid Dynamics and Combustion Technologies, University of Zaragoza, Spanish National Research Council, 50009 Zaragoza, Spain

Corresponding author: Mauro Carignano (mauroc@fceia.unr.edu.ar)

This work was supported in part by the Scholarship Program BECAR of Ministerio de Modernizacion of Argentina, under Project DPI2015-69286-C3-1-R and Project DPI2015-69286-C3-2-R (MINECO/FEDER) of the Spanish Government, in part by the European Commission H2020 through the Fuel Cell and Hydrogen Joint Undertaking Project under Project INN-BALANCE 735969 and Project REWIND LIFE13 ENV/ES/000280, in part by the Regional Government of Aragon to the Fluid Mechanics for a Clean Energy Research Group of LIFTEC under Grant T01_17R, in part by the Spanish State Research Agency through the Marí de Maeztu Seal of Excellence to IRI under Grant MDM-2016-0656, and in part by AGAUR of Generalitat de Catalunya through the Advanced Control Systems (SAC) Group under Grant 2017 SGR 482.

ABSTRACT The energy management strategy plays a major role in hybrid platforms powered by fuel cells (FCs) and batteries. This paper presents an assessment of energy management focused on fuel economy and battery degradation. Particularly, a proposed heuristic strategy and the widely known equivalent consumption minimization strategy are compared with the optimal solution obtained offline via dynamic programming. The case study is based on a real FC hybrid vehicle. Accordingly, the powertrain model of the vehicle used for the simulations is validated experimentally, and the profile of the power demand is measured from the real application. The results show that the proposed strategy offers the same performance as the equivalent consumption minimization strategy when the battery degradation is prioritized, and in comparison with the optimal off-line solution, it can be seen that there is still margin for improvement in terms of battery degradation.

INDEX TERMS Hybrid vehicle, fuel cell, battery degradation, energy management strategy, optimal strategy.

I. INTRODUCTION

Nowadays, Fuel Cell Hybrid Vehicles (FCHV) represent a solution of increasing interest for car manufacturers. Some examples are: Hyundai (TUCSON), General Motors (Chevrolet Equinox), Honda (FCX-V4 and FCX Clarity), Toyota (Toyota Mirai) and Volkswagen (Passat Lingyu). Nevertheless, some issues associated with hydrogen (H_2) production, distribution and storage, and fuel cell cost and lifetime, have to be improved to make this technology more profitable and affordable. A complete description of characteristics and challenges of FCHV are presented in [1]. Fuel Cells (FC) offer two main advantages compared with internal combustion engines: higher efficiency and zero emissions from the onboard source of power. However, FCs present some limitations associated with their slow transient response, which must be taken into account to avoid premature degradation. The reported literature points out that fast power variations cause conditions that promote the damage of the FC [2]–[4]. To cope with highly changing power profiles, FCHVs incorporate an energy storage system. Additionally, this energy storage system allows to recover energy from braking. In most cases, a battery is adopted for such purpose, but also, if the battery size is large enough, it is possible to propel the vehicle during a long period without using the FC. In these cases, the vehicle can be recharged from the electrical grid, and the FC allows to extend the vehicle autonomy. These vehicles are known as plug-in or range extender hybrid vehicles. Usually, they operate using only the battery until a certain level of charge, and then turn on the FC to supply electric energy to the vehicle and/or recharge the battery.

The energy management strategy (EMS) in FCHV affects both global efficiency and lifetime of the components. A review of EMS for FCHV presented in [1] points out that the Equivalent Consumption Minimization Strategy (ECMS),

based on a local optimization, is the most outstanding strategy. A complete description of the ECMS for FC vehicles is presented in [5]. In contrast to optimization approaches, heuristic strategies offer, in general, an acceptable performance and lower computational burden, which makes them more suitable for real-time applications. An heuristic strategy based on a FC map efficiency is presented in [6], while Hong-Wen *et al.* [7] and Yu *et al.* [8] present a comparison among different EMS including the ECMS.

Concerning the criteria chosen to develop and adjust the EMS, minimization of fuel consumption is the most widely used election, as shown in the previous works. It is because, in most hybrid platforms, the operating costs associated with fuel consumption represent a highest percentage among the overall cost [9]. However, costs associated with some components with a relatively short lifetime, as the battery and/or the FC, also represent a significant percentage of the total cost [10]. Depending on the type of hybrid platform, the battery cost can reach one-third of the total vehicle price [9], [11]. In case of FCHV, as the estimated lifetime of the battery is lower than the vehicle lifetime, it seems reasonable to include this aspect in the energy management issue. Accordingly, a fair comparison of the EMSs should take into account not only the H_2 consumption, but also the reduction of the battery lifetime. In this sense, Kelouwani *et al.* [12] present an anticipatory and real-time blended-mode EMS for battery life preservation. Although many works address the energy management for FCHVs, only some of them include the battery degradation, but comparisons with the optimal strategy are usually not presented. Odeim *et al.* [13] show the comparison between the optimal offline EMS, oriented only towards minimizing hydrogen consumption, and a real-time strategy based on multiobjective genetic algorithms. The result shows a dramatical improvement on the system durability at expense of a slightly higher hydrogen consumption than the offline optimum. However, to the best of our knowledge, there is not in the literature any work aimed to show the degree of optimality of the EMS in FC/Battery hybrid vehicles, where consumption and battery degradation are simultaneously set as objectives. This comparison is useful to determine the margin for improvement currently available.

An assessment of the EMS for a FCHV is presented in this work. Specifically an heuristic EMS is proposed, and the performance is compared to the results obtained with the ECMS and the optimal strategy, obtained offline via dynamic programming. The performance and the adjustments of the strategies are evaluated in terms of the fuel consumption and the battery degradation. The latter is computed through an explicit degradation model. The case study concerns to a real application, currently in operation. Accordingly, data from the real vehicle were used to create and validate the models, and to obtain the real profile of power demand. The performance of the strategies is evaluated by simulation, and then, the proposed strategy is implemented in the real vehicle. The rest of the paper is organized as follows: in Section II the FCHV and the models used are presented; Section III describes the EMSs; in Section IV, the simulation and experimental results are presented; and finally the conclusions and a prospective are drawn in Section V.

TABLE 1. Characteristics of the vehicle.

Chassis	Weight	850 Kg
	Transmission	4x4, One Motor
Induction Motor	Nominal Power	7.5 kW
	Max. Power	32 kW
	Converter	72 V, 550 A
Lead-Acid Battery	Nominal Voltage	72 V
	Capacity	225 Ah
PEM Fuel Cell	Nominal Model	Horizon^{TM} H-3000
	Rated Power	3000 W
	Rated Voltage	43.2 V

II. VEHICLE MODEL

The study presented in this work is based on tests performed with the vehicle shown in Fig. 1-a. This vehicle is used daily in an eco-friendly vineyard, which produces electricity and hydrogen from solar energy [14]. The vehicle was originally pure electric [15], designed for bumpy and irregular terrain, typically for agricultural and industrial tasks. In order to extend its autonomy, a Proton Exchange Membrane FC was added (see Section II-C). The original vehicle has 41 MJ of electric energy available from the batteries, and this amount was increased to around 73 MJ with the addition of a FC system, which notably extended its autonomy (up to a 78 %). Table 1 sumarizes some caracterirtics of the modified vehicle. Detailed information about this and the remodeling process can be found in [16].

According to the configuration shown in Fig. 1-b, the power at the wheels is provided by the Electric Machine (EM) through the Differential. The EM can also work as generator to recover energy from braking. The vehicle has three gears with manual shift, and the regenerative braking only works in the lowest gear. The EM is connected to the direct current bus (DC-BUS) through an electronic converter. Then, the FC delivers power through the boost converter to the DC-BUS. Note that the voltage of the DC-BUS is determined by the battery voltage.

The model of the powertrain used to evaluate the energy consumption and the power demands is focused on the efficiency of components, neglecting most of the component dynamics. Accordingly, the electronic converters and the EM are included in the model through their efficiencies. In the following sections, the battery and the FC model are described and the FCHV model used for the simulation is presented.

A. BATTERY MODEL

The model used to reproduce the dynamic behavior of the battery is based on the works by Tremblay and Dessaint [17] and Cabello *et al.* [18]. It is equivalent to the widely used first-order resistance capacitance model [19]. The terminal voltage is given by the following expression,

$$U_{BAT}(k) = U_{BAT,oc}(k) - R_{BAT}\, I_{BAT}(k), \tag{1}$$

(a)

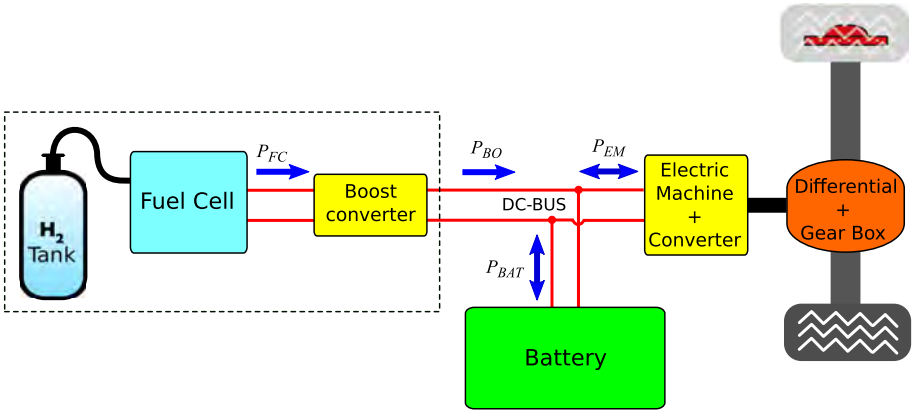

(b)

FIGURE 1. (a) FCHV vehicle used as case study; (b) final configuration, squared in dotted line the FC system added.

where k stands for the sampling time, $U_{BAT,oc}$ is the open-circuit voltage, R_{BAT} is the internal resistance and I_{BAT} is the current flowing through the battery. Then, $U_{BAT,oc}$ depends on the battery state of charge (SOC), and on the filtered current (I^*_{BAT}) as follows:

$$U_{BAT,oc}(k) = U_{BAT,0} - K_1(1 - SOC(k)) - K_2\, I^*_{BAT}(k), \tag{2}$$

where $U_{BAT,0}$, K_1 and K_2 are adjustable parameters. The SOC dynamics can be expressed as follows,

$$SOC(k+1) = SOC(k) - \frac{I_{BAT}(k)\, t_s}{Q_{BAT,0}}. \tag{3}$$

where t_s is the time interval of the discretization and $Q_{BAT,0}$ is the capacity of the battery. According to this expression, the current in the battery is considered positive for discharging, and negative for charging. The filtered current I^*_{BAT} is computed through a first order filter,

$$I^*_{BAT}(k) = \frac{I^*_{BAT}(k-1)\,\tau_{BAT} + I_{BAT}(k)\, t_s}{\tau_{BAT} + t_s}, \tag{4}$$

where τ_{BAT} is the battery time constant. The battery current can be computed from the power demand,

$$I_{BAT}(k) = \frac{U_{BAT,oc}(k) - (U^2_{BAT,oc}(k) - 4P_{BAT}(k)R_{BAT})^{0.5}}{2\, R_{BAT}}. \tag{5}$$

The battery of this vehicle is composed of 12 sealed lead-acid units (also known as gel cell), connected in series. Each unit has a nominal voltage of 6 V and a capacity 200 Ah to 0.1 C-rate (AGM, model HDKEV6V [20]). To determine the parameters of the battery model, two experiments were performed. First, a discharge from full to empty with a constant current of 6A. It was used to determine $U_{BAT,0}$, K_1 and $Q_{BAT,0}$. Then, a profile of current and voltage from the battery was measured with the vehicle in operation, and they were used to determine R_{BAT}, K_2 and τ_{BAT}. In both cases, least squares criteria was used to adjust the parameters to the experiments. We were specially interested in obtaining a good fit of the battery model in the range of SOC where the vehicle operates most of the time. This range is from 0.5 to 0.8.

The following parameters were obtained from the previous tests: $U_{BAT,0} = 75.8\,V$, $K_1 = 9.61\,V$, $Q_{BAT,0} = 180\,Ah$, $R_{BAT} = 0.0377\,\Omega$, $K_2 = 0.0241\,\Omega$ and $\tau_{BAT} = 45\,s$. Fig. 2-a,

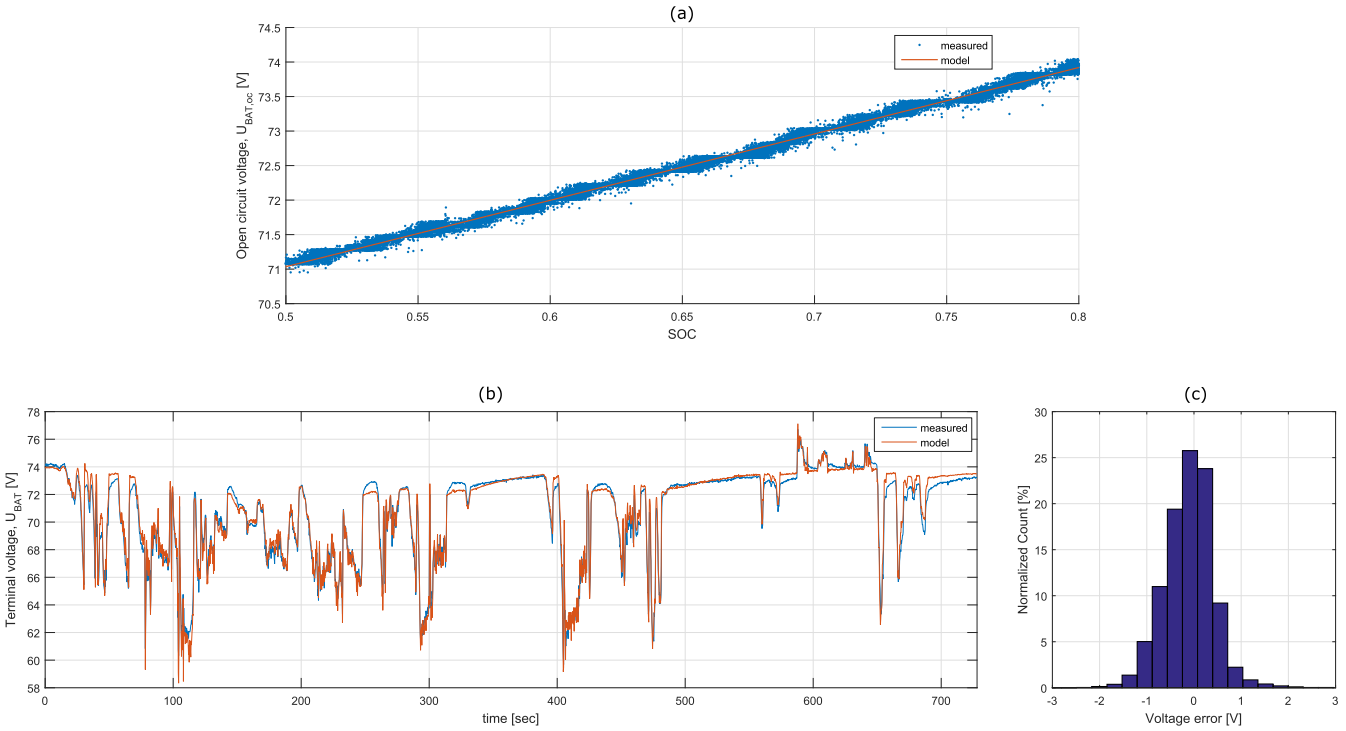

FIGURE 2. (a) Evolution of the battery voltage as function of SOC in the discharge test, (b) behavior of battery voltage under dynamic conditions, and (c) histogram of voltage error.

shows the evolution of the voltage reproduced by the model and the experimental value during a discharge test. As it can be seen, the linear model offers a good approximation to the battery behavior, while Fig. 2-b shows the evolution of the voltage reproduced by the model and the experimental values during a test in dynamic conditions. Fig. 2-c shows the difference between the measured voltage and the one obtained with the model, which is lower than 1 V in 95 % of the points.

B. BATTERY AGING

As it was mentioned in the introduction, the assessment of the EMS presented in this work focuses not only on fuel economy but also on battery degradation. For this purpose, it is required to quantify the damage produced in the battery by a given current profile.

Typical data offered by battery manufacturers provide information about how many repetitive cycles can withstand at a given depth of discharge (DOD), under controlled conditions (current and temperature). However, these conditions are very different from those suffered by a battery in a HEV under real driving conditions. The literature reports different methods to quantify lifetime of the batteries under dynamic conditions. In this case the method proposed by the Ohio State University for electric vehicles will be used [21]–[24]. This is based on the concept of *Ah-throughput*, which assumes that there is an amount of charge that can circulate through the battery (on charge or discharge situations) before reaching its end of life (EOL). The model takes also into account the effect of the operating temperature, the DOD and the C-rate.

For a given current in the battery expressed in Amperes, the C-rate index is defined as:

$$C_{rate} = \frac{|I_{BAT}|}{Q_{BAT}}, \tag{6}$$

where Q_{BAT} is the nominal capacity of the battery expressed in Ah. The information provided by manufacturers is normally expressed in terms of C_{rate}, and tests to evaluate durability are usually performed at $C_{rate} = 1$ or lower. The DOD is complementary of the SOC, i.e. $DOD = 1 - SOC$. High values of C_{rate} and high values of DOD contribute to accelerate the battery deterioration. Another factor that contributes in the same sense is operating the battery at high temperature.

For a given battery, the nominal *Ah-throughput* is defined as:

$$Ah_{nom} = \int_0^{EOL} |I_{nom}(\tau)|\, d\tau. \tag{7}$$

Typically, the nominal condition refers to $C_{rate} = 1$, $DOD = 100\%$ and temperature of $25^o\ C$. Then, for a certain current profile, the effective *Ah-throughput* is computed as:

$$Ah_{eff}(t) = \int_0^{t} |I_{BAT}(\tau)|\, \sigma(\tau)\, d\tau, \tag{8}$$

where σ is a weight factor named severity factor, which depends on the C_{rate}, the DOD and the battery temperature. The severity factor is always greater than 1, and it increases

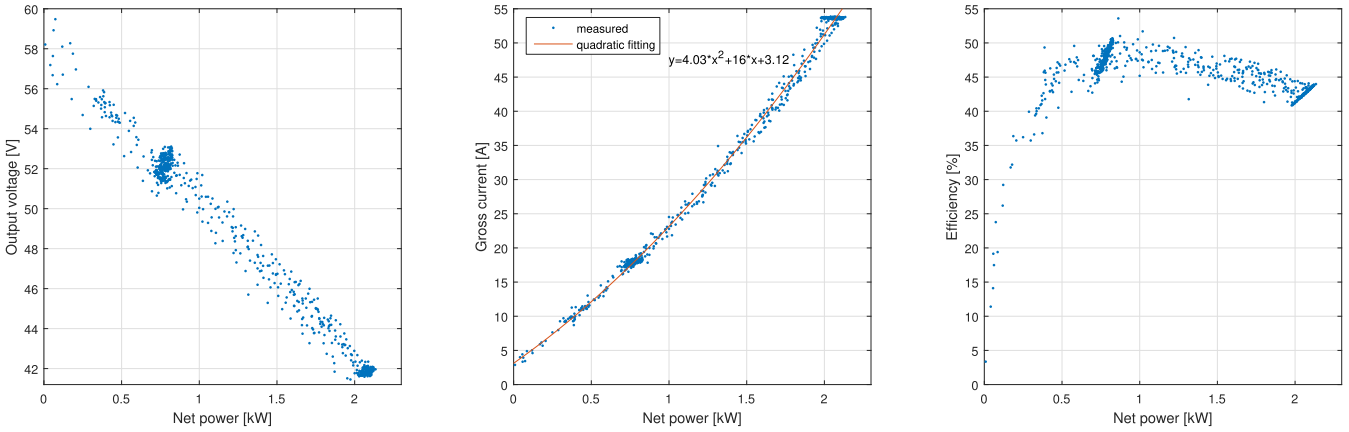

FIGURE 3. Experimental fuel cell performance analysis and curve fitting.

with C_{rate}, DOD and temperature. In the case under study, the battery is large enough to hold the C_{rate} below 2 in operation, which produces a negligible effect on the severity factor [25]. Then, as will be seen in the results, the trajectory of the DOD is slightly changed by the EMSs, therefore, and for the purposes of these comparisons, the variation of σ with the DOD is neglected. The effect of the DOD must be considered only if an accurate estimation of the battery lifetime is required. Finally, the effect of temperature on the severity factor is neglected in our case due to the small variation of the battery temperature observed during the tests. If this were not the case, a thermal model would be necessary. According to the previous considerations, the severity in our model of degradation is considered constant, and equal to 1.

Lastly, the fraction of battery life consumed is estimated as:

$$BAT_{life}(t) = \frac{Ah_{eff}(t)}{Ah_{nom}}. \tag{9}$$

Aging is cumulative, and when it equals 1, the battery has reached its EOL and must be replaced. Therefore, a reduction in the Ah_{eff} leads to extend the battery life-time. Finally, it is worth mention that although the models presented are used in this work for a lead-acid battery, they have been also used for Li-ion and NiMH batteries in the aforementioned literature.

C. FUEL CELL MODEL

Hydrogen FCs are used to generate electricity from an electrochemical reaction between oxygen and H_2. Despite the existence of many types of FCs, proton exchange membrane (PEM) FCs are the most common in automotive applications [1]. In this case, the vehicle was equipped with a Horizon^{TM} H-3000 open cathode PEMFC, composed by 72 cells and a maximum power of 3000W. The original control was eliminated, and replaced by our own system that allows hydrogen recirculation through a Venturi ejector. For the purposes of this work, the FC model is reduced to a quasistatic one that includes a fuel consumption map and a set of constraints. Although the FC is able to deliver up to 3000 W, when the stack temperature is not high enough the stack voltage decreases, and the FC is not able to reach its maximum power. In these cases, a fail by low voltage might appear, and the FC would interrupt its operation. To avoid this situations, the FC is operated up to a maximum of 2100 W. On the other hand, the minimum power allowed to the FC is 0, meaning that the FC is in standby. Note that FC power refers to the net power, i.e. the gross power minus the power of auxiliary components. Figure 3 shows the performance of the FC in operation under real dynamic conditions. The high density of sample points around 750 and 2100 W is due to the particular EMS used during the test.

As it was mentioned in the introduction, the variations of the power delivered by the FC are limited in order to avoid premature aging. Currently it is not entirely clear how to establish such limits accurately. Quantifying FC degradation is a complex task, mainly because the degradation rate strongly depends on the internal conditions. Local starvation and over-voltage can occur when the catalytic layers of the FC are not supplied with the proper amount of reactants. Although some authors do not consider power rate constraints in the fuel cell [12], [26]–[28], generally, a fixed rate condition is adopted. Accordingly, a wide range of power rate constraints can be found in the literature. The most conservative values, reported by Alfonso *et al.* [29] and Valverde *et al.* [30], use a maximum rate allowed around 2% of its maximum power per second. Alternatively, other authors adopted higher values between 5% and 15% [5], [6], [31]–[33], 20% [34] and 40% [35]. In this work, a maximum of 10 % per second for rising, and 30 % per second for falling of the maximum FC power (3000w) are assumed.

The power gradient in the FC is:

$$\Delta P_{FC}(k) = \frac{P_{FC}(k) - P_{FC}(k-1)}{t_s}, \tag{10}$$

where $P_{FC}(k)$ is the power delivered by the FC. This variable, as will be seen later, is the control input computed by the EMS. Then, control input is constrained as follows:

$$0 \leq P_{FC}(k) \leq 2100, \tag{11}$$

$$-900 \leq \Delta P_{FC}(k) \leq 300. \tag{12}$$

Notice that (12) depends on the previous and the actual power values. An option to deal with these constraints is to consider the power in the FC as a state variable with the following state equation:

$$x_{FC}(k+1) = P_{FC}(k). \tag{13}$$

Now, the constraint (12) is state-dependent. This constraint, in general, imposes hard constraints for the EMS, affecting noticeably the vehicle performance.

Finally, the H_2 consumption can be obtained from the gross current. The instantaneous fuel consumption can be computed as follows [36]:

$$\dot{m}_{H_2} = I_{FC,gross} \frac{0.03761}{3600} N_{cell}, \tag{14}$$

where $\dot{m}_{H_2}$ is the H_2 mass flow rate in grams per second, $I_{FC,gross}$ is the gross current (i.e. stack current) in amperes, and N_{cell} is the number of cells of the FC stack. So far, only the H_2 that reacts has been considered. Another factor that contributes to the consumption, but to a lesser extent, is the H_2 released by purges. The amount of H_2 released in purges is difficult to estimate or reproduce through a model. Assuming that this amount of fuel does not depend on the EMS adopted, the comparison of the consumption is performed counting only the H_2 that reacts in the cells of the stack.

D. BOOST CONVERTER

As it is shown in Fig. 1-b, a boost converter is required to control the power flow from the FC to the DC-BUS. The FC voltage varies between 35 and 70 V, while the voltage of the DC-BUS is given by the battery voltage. The boost converter used in the vehicle is the model CH100105F-SU from Zahn Electronics™. It can handle input voltages from 24 to 78 V and currents up to 105 A; at the output it can generate voltages from 26 to 80 V and currents up to 96 A. It is equipped with a LC filter that softens the FC voltage. Figure 4 shows its performance under real dynamic conditions. For the purpose of powertrain model, the boost converter efficiency is modeled through the static equation shown in this figure.

It is worth clarifying that although the efficiency of the boost converter is affected by the input/output voltage, in this case can be neglected due to i) the output voltage (battery voltage) has not high variation, and ii) the input voltage (FC voltage) is function of the power delivered. So, the efficiency curve obtained for the boost converter has a connection with the FC performance.

E. FCHV MODEL

The complete power balance (Fig. 1-b) in the DC-BUS leads to:

$$P_{BAT}(k) + P_{BO}(k) - P_{EM}(k) = 0 \tag{15}$$

where $P_{BO}(k) = P_{FC}(k)\,\eta_{BO}(k)$ is the power delivered by the boost converter. According to eq. (15), and assuming

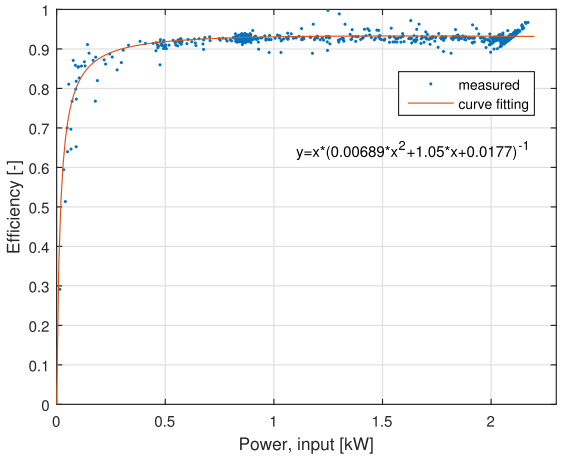

FIGURE 4. Boost converter performance and curve fitting.

that $P_{EM}(k)$ is given by the demand, the propulsion system has one degree of freedom. As it was mentioned, $P_{FC}(k)$ is chosen as control input and is defined by the EMS. On the other hand, $P_{EM}(k)$ depends on the required power, given in general by a driving cycle. In this work, the power flow in the EM is measured, and it is used as input. Figure 5 shows a schematic representation of the causal model used to perform the simulations.

III. ENERGY MANAGEMENT

The FCHV presented in this work is used inside a vineyard. The electrical energy is produced from renewable sources and it is used to produce H_2 by hydrolysis. From an energetic point of view, the most efficient alternative to propel the vehicle is by using the battery as much as possible, avoiding to use the FC. The double conversion from electricity to hydrogen, and vice versa, leads to a total efficiency very low. However, as it was mentioned before, the FC was mainly added with the aim of extending its autonomy, turning it into a range extender vehicle. Furthermore, incorporating the FC, as will be seen later, allows to reduce the stress on the battery. Accordingly, it was decided that the FCHV will operate in full battery mode, until the SOC reaches 95%. Then, the FC is switched on and the vehicle operates in *shared mode*. Below 40% of SOC, the FC operates at maximum power in order to recharge the battery. It is clear that the modes full battery and FC at maximum power do not require an EMS. Alternatively, in the *shared mode*, the power delivered by the FC must be defined by the EMS. Accordingly, the range of SOC where the EMS operates is from 40 % to 95%. The following sections describe the EMSs analyzed in this work.

A. BOUNDED LOAD FOLLOWING STRATEGY

The strategy proposed in this work, named Bounded Load Following Strategy (BLFS), was designed to operate the FC at high efficiency, but also to alleviate the current that flows through the battery. To operate the FC at high efficiency, the power is bounded by two limits, which are adjusted according to the efficiency curve of the FC. Then, to alleviate

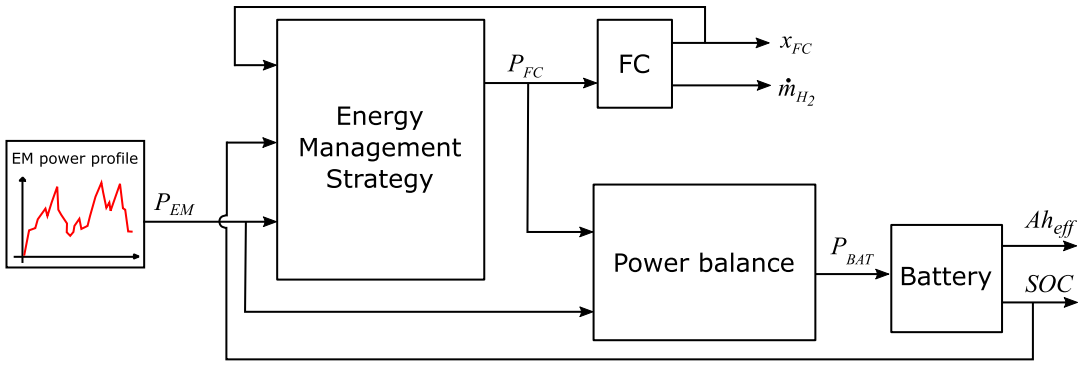

FIGURE 5. Schematic representation of the model used to perform the simulations.

the current that flows through the battery, a tracking of the power demand is proposed. It means that the power delivered by the FC will increase if the power demanded for the EM increases, and vice verse. In this way, the power flow in the battery decreases. Notice that this purpose is strongly affected by the FC power gradient constraints and the variations in the power demanded of the EM according to the driver behavior.

The first variable computed in the BLFS is named tracking power (P_{tkg}). It is computed through the power demanded by the EM from the DC-BUS and the boost converter efficiency,

$$P_{tkg}(k) = P_{EM}(k)\,\eta_{BO}^{-1}, \tag{16}$$

where $P_{EM}(k)$ is measured and η_{BO} is assumed to be constant, and equal to 0.94. Then, in order to operate the FC in a feasible and efficient zone, the tracking power is bounded as follows,

$$P_{bnd}(k) = \max\{\min\{P_{tkg}(k), P_{FC,hi}\}, P_{FC,lo}\}, \tag{17}$$

where $P_{FC,hi}$ and $P_{FC,lo}$ are the high and low limits respectively, $0 < P_{FC,lo} < P_{FC,hi} < 2100$. The bounded power ($P_{bnd}$) is an internal variable of the BLFS. Finally, the power assigned to the FC has to be constrained according to the allowed power gradient. Taking into account the power gradient constraints presented in section II-E, the power assigned to the FC results:

$$P_{FC}(k) = \max\{\min\{P_{bnd}(k), P_{FC}(k-1) + 300\,t_s\}, P_{FC}(k-1) - 900\,t_s\}. \tag{18}$$

As can be seen, the proposed strategy has only two adjustment parameters: $P_{FC,hi}$ and $P_{FC,lo}$. Figure 6 shows the block diagram of the strategy.

B. STRATEGIES BASED ON OPTIMIZATION

This section presents both the Equivalent Consumption Minimization Strategy (ECMS) and the formulation of the global optimization problem. The ECMS is an online EMS that consists in solving a local optimization problem to find the control input [37]. This strategy was analyzed in applications with IC Engine-Battery powered hybrid vehicles [38], [39], but it was also studied in FCHV [1]. The reported literature shows that the ECMS produces results close to the optimal solution in most of the hybrid platforms, except in the cases of active state-dependent constraints [33], [40].

In this case, the local optimization problem that the ECMS solves to find the control input ($u(k)$) is associated with the instantaneous H_2 consumption and with the battery current,

$$u(k) = \arg \min_{u(k)\subseteq U(k)} \{\dot{m}_{H_2}(u(k)) + s_{eq}\, I_{BAT}(u(k), SOC(k), I^*_{BAT}(k), k)\}, \tag{19}$$

where $U(k)$ is the set of feasible control inputs, established by the component constraints, and s_{eq} is the equivalence factor used to convert the electric consumption from the battery to an equivalent H_2 consumption. The equivalence factor can vary as a function of the SOC, aiming to maintain the SOC close to a certain reference value; or it can be considered constant. It is worth noticing that a variable equivalence factor does not lead to better results in terms of performance, but it does increase the robustness of the EMS again in different power demand profiles. In this work, s_{eq} is considered constant, and it is adjusted offline by iteration to fulfill the boundary SOC condition. Returning to the expression (19), $\dot{m}_{H_2}(u(k))$ is proportional to the FC gross current, therefore, the following expression is equivalent,

$$u(k) = \arg \min_{u(k)\subseteq U(k)} \{I_{FC,gross}(u(k)) + s_{eq}\, I_{BAT}(u(k), k)\}. \tag{20}$$

To simplify the notation, the dependency of the I_{BAT} on SOC and I^*_{BAT} has been omitted. Finally, in order to consider the battery stress in the formulation of the ECMS, a third term is added in the minimization, and a weight factor is also introduced,

$$u(k) = \arg \min_{u(k)\subseteq U(k)} \Big\{(1-\alpha)\,\{I_{FC,gross}(u(k)) + s_{eq}\, I_{BAT}(u(k), k)\} + \alpha\ |\, I_{BAT}(u(k), k)\,|\Big\}. \tag{21}$$

The weight factor allows to vary the performance of the strategy from maximum fuel economy to maximum care of the battery as α varies from 0 to 1.

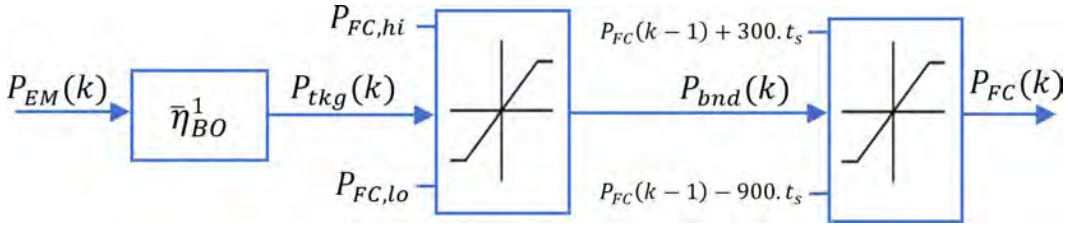

FIGURE 6. Block Diagram of the BLFS.

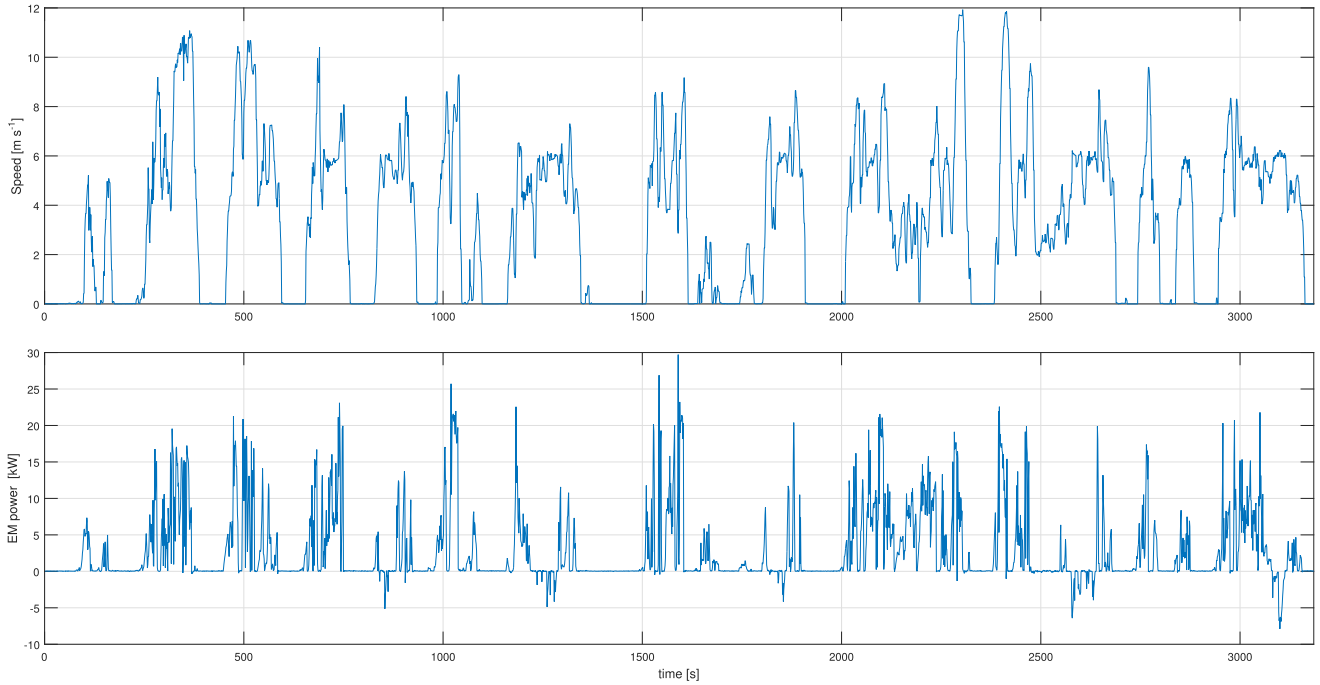

FIGURE 7. Driving cycle and power profile used to evaluate the strategies.

Notice that Eq. (20) is a particular case of (21) when $\alpha = 0$.

The optimal EMS can be obtained as the solution of the global optimization problem, which can be formulated as follows: to find the sequence of control input $u(k)$, $k = 1, ..., N$, that minimize,

$$J = \sum_{k=1}^{N-1} (1-\alpha)\, I_{FC,gross}(u(k), k) \tag{22}$$

$$+\alpha \mid I_{BAT}(\boldsymbol{x}(k), u(k), k) \mid, \tag{23}$$

subject to,

$$0 \leq u(k) \leq 2100, \tag{24}$$

$$-900 \leq \Delta P_{FC}(\boldsymbol{x}(k), u(k)) \leq 300, \tag{25}$$

$$\boldsymbol{x}(k+1) = \mathbf{f}(\boldsymbol{x}(k), u(k), k), \tag{26}$$

$$\boldsymbol{x}(1) = \boldsymbol{x_0}, \tag{27}$$

$$\boldsymbol{x}(N) = \boldsymbol{x_f}, \tag{28}$$

where, $\boldsymbol{x}(k) \triangleq [SOC(k), I^*_{BAT}(k), x_{FC}(k)]$ is the state vector, $u(k) \triangleq P_{FC}(k)$ is the control input, and $\mathbf{f}$ is the system dynamics defined by (3)-(4)-(13). The first term in the summation accounts for fuel consumption, while the second represents the usage of the battery. The weight factor α has the same meaning that the one in the ECMS formulation. Equation (28) is the boundary condition associated to the final value of the state variables. Specifically in this case, the SOC is constrained, while I^*_{BAT} and x_{FC} are free. To solve this problem, the method of dynamic programming was adopted. It guarantees the optimal solution, even in presence of active state-dependent constraints [41]. As can be observed, the optimization problem has three state variables, which implies a hard computational cost for the dynamic programming method. A vectorized implementation is adopted following the guidelines given in [42].

IV. SIMULATION AND EXPERIMENTAL RESULTS

The proposed strategy is evaluated by simulation under a real power demand profile. The results are compared with those obtained with the ECMS and the optimal offline solution.

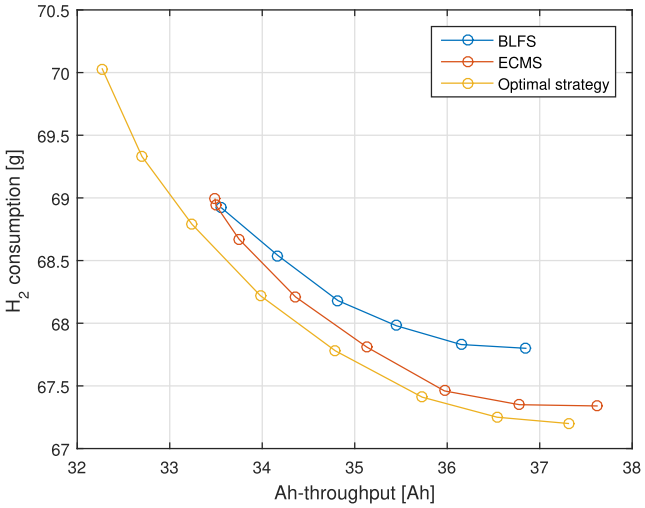

FIGURE 8. Performance of the strategies for different adjustments, expressed in terms of hydrogen consumption and battery degradation.

Finally, the proposed strategy is implemented in the real FCHV and the experimental results are presented. The experimental comparison between them was not addressed because our impossibility to repeat the same driving conditions at each test.

A. POWER DEMAND AND ADJUSTMENT OF THE STRATEGIES

The use of realistic driving conditions is essential to determine the effectiveness of a control strategy. In this work, with the aim of building a representative power demand profile, the power flow in the EM was recorded along different common trips around the vineyard. This profile, shown in Fig. 7, is used to evaluate the performance of the strategies in the simulations.

Regarding the EMS parameter tunning, they are swept in order to obtain the set of different performances, considering the constraints associated with the SOC at the end of the cycle. Specifically, the initial and final SOC adopted are $SOC(0) = 0.75$ and $SOC(N) = 0.6254$. The proposed final value of SOC was obtained using the driving cycle presented before, starting from $SOC(0) = 0.75$, and with the FC operating at constant power equal to 1200 W. This average power in the FC guarantees the levels of autonomy pretended in the vineyard. Notice that the fixed boundary condition associated to the SOC at the end of the cycle leads to a fair comparison between the strategies because avoids the compensation of the fuel consumption due to differences in the final SOC value.

B. RESULTS

We are interested in comparing the performance of the strategies in terms of fuel consumption and battery damage. Therefore, the H_2 mass consumed, in grams [g], and the total electric charge through the battery, expressed in Ampere-hour [Ah], are adopted as performance indicators.

TABLE 2. Performance obtained with the BLFS using different values of $P_{FC,low}$ and $P_{FC,hi}$.

$P_{FC,low}$ $[W]$	1000	950	900	850	800	750
$P_{FC,hi}$ $[W]$	1580	1680	1785	1885	1990	2100
H_2 Consumption $[g]$	**67.80**	67.83	67.98	68.18	68.54	68.92
Ah-throughput $[Ah]$	36.85	36.15	35.45	34.82	34.17	**33.56**

The last one is the effective Ah-throughput, introduced in Section II-B with expression (8).

Figure 8 shows the performance of the strategies, and Tables 2, 3 and 4 summarize these results plus the corresponding parameters. Bold numbers in the tables indicate the minimum value of consumption and the minimum value of Ah-throughput achievable with each strategy. Firstly, it can be seen that for real-time strategies (ECMS, BLFS), a reduction of around 10 % in battery damage is possible with an increment of around 2% in fuel consumption. Then, when fuel economy is prioritized, the minimum consumption obtained with the proposed strategy is only 0.6 % above the minimum consumption achieved with the optimal strategy, while the damage produced in the battery is favorable with the BLFS.

Regarding the ECMS in terms of H_2 consumption, when the same is prioritized (i.e. $\alpha = 0$), it is even closer to the optimal solution compared to BLFS. However, when the damage produced in the battery is prioritized, the proposed strategy reaches the same performance, in terms of fuel consumption and Ah-throughput, as the ECMS. In this sense, the optimal strategy can reduce even more the damage on the battery, but increase the fuel consumption.

Finally, it is worth noticing that for the ECMS, the maximum value of α has been fixed in 0.5. Further increases do not produce appreciable changes in the results. On the contrary, although it has not been included in the results, increasings α beyond 0.5 in the optimal strategy reduces even more the battery damage.

For a better understanding of the strategies, Figure 9 shows how the FC and the battery operate. In these results, three strategies were fitted to obtain the maximum care of the battery. As can be seen, ECMS and BLFS operate the FC, and consequently, the battery, in a very similar way. On the other hand, with the optimal strategy there are two main differences. First, in the case of propulsion (left figures), the FC rises the power before the EM demand, and in case of regenerative braking (right figures), the FC reduces the power before the EM generation. This behavior of the optimal strategy reduces the effective Ah-throughput in the battery. Secondary, if the vehicle is stopped, with the optimal strategy, the FC provides lower power than with the real-time strategies.

So far, three strategies have been presented and analyzed by simulation. Only the ECMS and the BLFS can be implemented in real-time. After analyzing the simulation results, it seems reasonable to prioritize the battery damage at expense of a slight increase of fuel consumption. As has

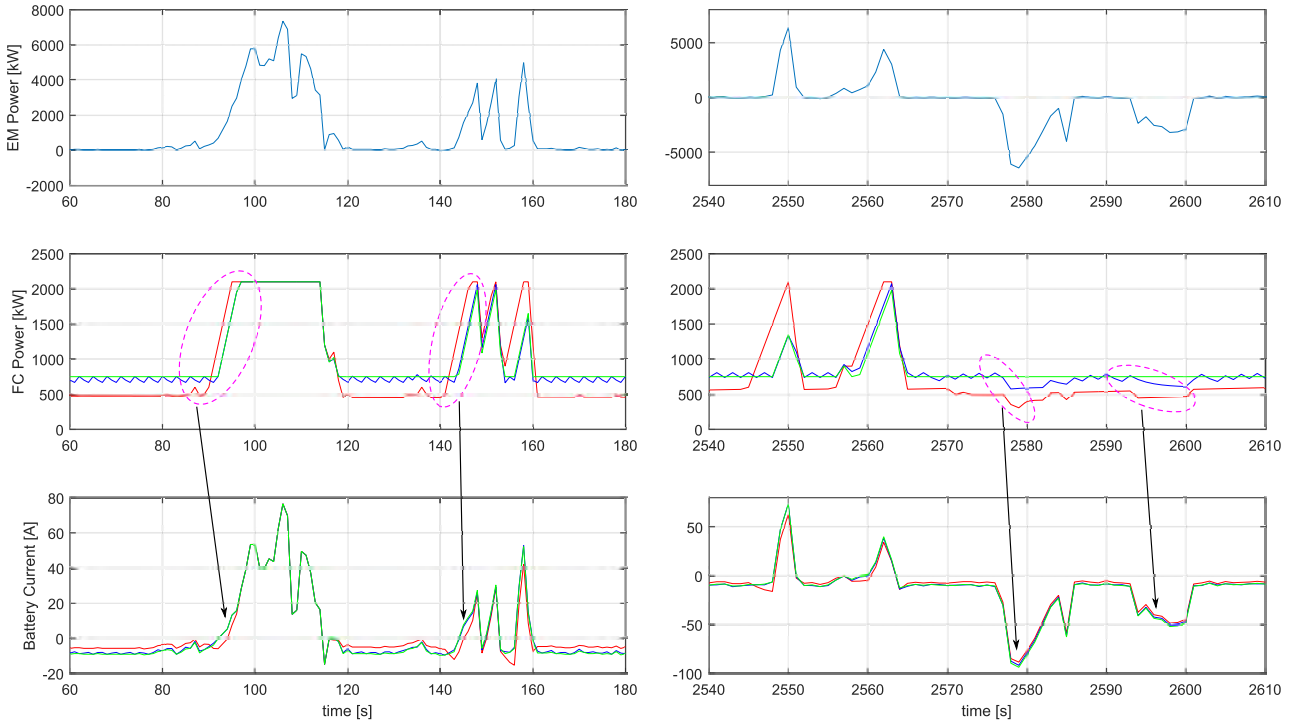

FIGURE 9. Segments of the cycle with the Optimal (red), ECMS (blue) and BLFS (green) strategies.

TABLE 3. Performance achieved with the ECMS using different values of s_{eq} and α.

s_{eq} $[-]$	1.914	1.926	1.943	1.968	2.006	2.053	2.134	2.705
α $[-]$	0	0.05	0.10	0.15	0.20	0.25	0.30	0.5
H_2 Consumption $[g]$	**67.34**	67.35	67.46	67.81	68.21	68.67	68.94	68.99
Ah-throughput $[Ah]$	37.62	36.78	35.97	35.13	34.36	33.75	33.50	**33.49**

TABLE 4. Performances obtained with the optimal strategy using different values of α.

α $[-]$	0	0.05	0.10	0.15	0.20	0.25	0.30	0.5
H_2 Consumption $[g]$	**67.20**	67.25	67.41	67.78	68.22	68.79	69.33	70.03
Ah-throughput $[Ah]$	37.31	36.54	35.73	34.79	33.98	33.24	32.70	**32.27**

been previously discussed, when the damage of battery is prioritized, both ECMS and BLFS provide the same performances. From the point of view of the effort required to compute these strategies, neither of them seems to be highly demanding, although the ECMS has to solve (21), which may result more demanding than the set of operations from (16) to (18) required by BLFS. In this sense, and according with the computer mounted in the vehicle [16], both strategies could had been used in real time. In this case, the BLFS was finally adopted and implemented as EMS in the FCHV. The parameter used in this strategy corresponds to the performance that reduces the damage of the battery, i.e. $P_{FC,low} = 750\,W$ and $P_{FC,hi} = 2100\,W$. Figure 10, shows a segment of the data acquired during a real road test with the proposed strategy implemented. It can be observed how the FC 'follows' the power demanded by the EM. Some variables are low-pass filtered before been used in the EMS in order to clean them from noise.

V. CONCLUSIONS

An assessment of the energy management for a real fuel cell/battery hybrid vehicle has been performed in this work. Particularly, an heuristic strategy was proposed, and it was compared with two references: the widely known Equivalent Consumption Minimization Strategy and the optimal strategy, obtained offline via dynamic programming. Hydrogen consumption and battery degradation were the criteria used to adjust and evaluate the strategies. Results were obtained by simulations using a model of the FCHV built from the real vehicle and adjusted from real tests.

Results show that the proposed strategy provides a performance comparable to the ECMS, and particularly, when the damage of battery is prioritized, both strategies reach the same results. Regardless of the strategy finally adopted, it has been shown that a considerable reduction on battery damage can be achieved with relative low increment of fuel consumption. On the other hand, in comparison with the

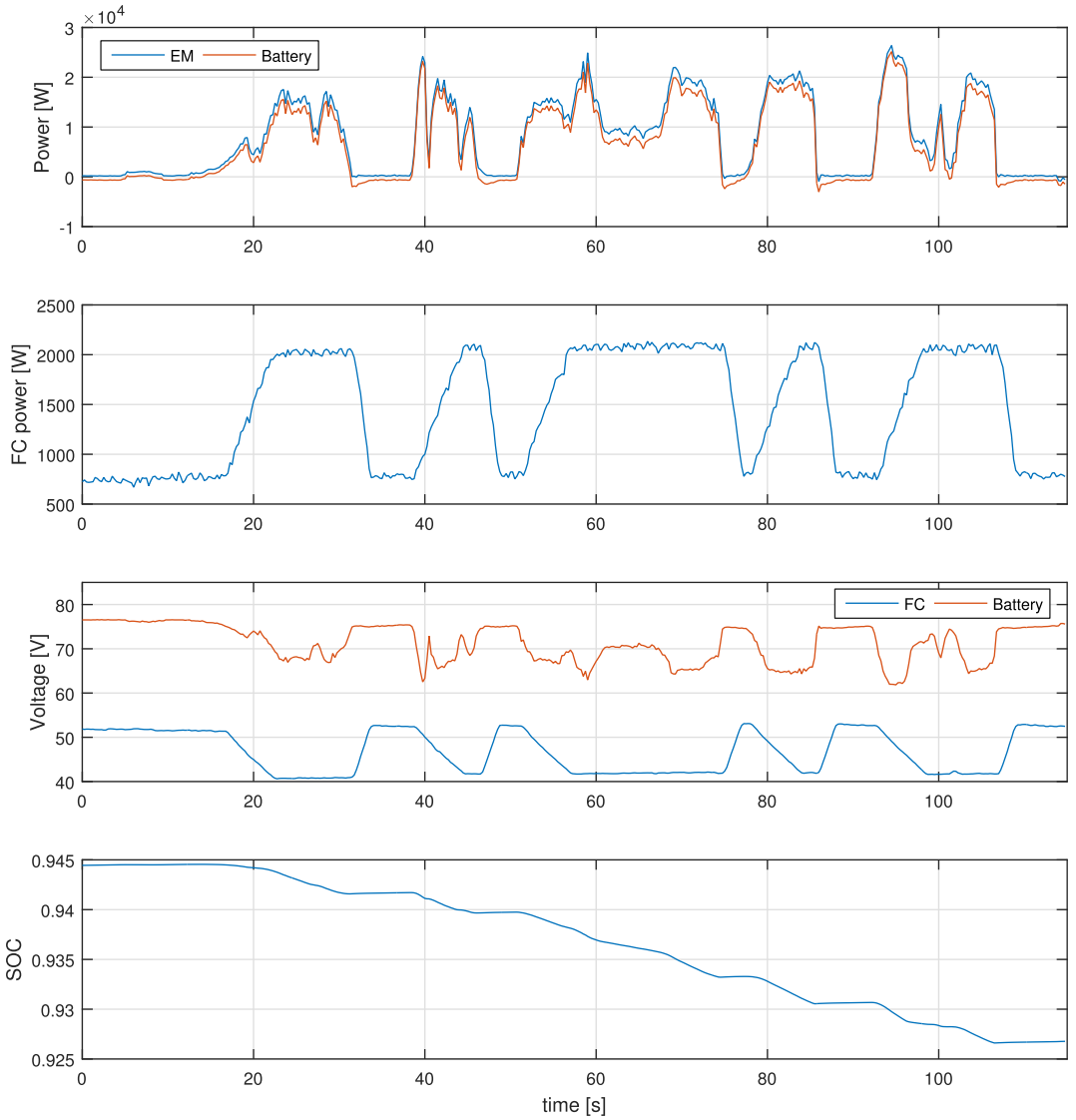

FIGURE 10. Segment of the data acquired from the FCHV operating with the BLFS implemented.

optimal strategy, both real-time strategies provide optimal results in term of fuel economy, with differences lower than 0.5%. However, if the maximum care of battery is pretended, there is still a margin for improvement of 4%. Regarding that, it must be considered that the optimal strategy knows the future in advance, and therefore it increases or reduces the FC power before a propulsion or a braking period, respectively, in order to alleviate the current flow through the battery. Accordingly, we think that the performance of the real-time strategies can be improved by including an estimation on the energy demand in a near future.

Nowadays, with FCHVs trying to gain a place in the automotive market, it is crucial to work not only on fuel economy, but also on the lifetime of its components, in order to make this platforms more affordable. In this sense, this work represents a contribution, and although the presented results correspond to a particular case (PEM Fuel Cell + Lead-Acid Battery), the proposed methodology is general, and can be applied in a wide range of scenarios of energy management in fuel cell/battery hybrid vehicles.

REFERENCES

[1] N. Sulaiman, M. A. Hannan, A. Mohamed, E. H. Majlan, and W. R. W. Daud, "A review on energy management system for fuel cell hybrid electric vehicle: Issues and challenges," *Renew. Sustain. Energy Rev.*, vol. 52, pp. 802–814, Dec. 2015.

[2] S. Strahl, N. Gasamans, J. Llorca, and A. Husar, "Experimental analysis of a degraded open-cathode PEM fuel cell stack," *Int. J. Hydrogen Energy*, vol. 39, no. 10, pp. 5378–5387, 2014.

[3] R. Borup *et al.*, "Scientific aspects of polymer electrolyte fuel cell durability and degradation," *Chem. Rev.*, vol. 107, no. 10, pp. 3904–3951, 2007.

[4] M. Uchimura and S. S. Kocha, "The impact of cycle profile on PEMFC durability," *ECS Trans.*, vol. 11, no. 1, pp. 1215–1226, 2007.

[5] P. Rodatz, G. Paganelli, A. Sciarretta, and L. Guzzella, "Optimal power management of an experimental fuel cell/supercapacitor-powered hybrid vehicle," *Control Eng. Pract.*, vol. 13, no. 1, pp. 41–53, 2005.

[6] D. Feroldi, M. Serra, and J. Riera, "Energy management strategies based on efficiency map for fuel cell hybrid vehicles," *J. Power Sour.*, vol. 190, no. 2, pp. 387–401, 2009.
[7] H.-W. He, Y.-Q. Zhang, and F. Wan, "Control strategies design for a fuel cell hybrid electric vehicle," in *Proc. IEEE Vehicle Power Propuls. Conf.*, Sep. 2008, pp. 1–6.
[8] S. Yu, J. Zhang, and L. Wang, "Power management strategy with regenerative braking for fuel cell hybrid electric vehicle," in *Proc. Asia–Pacific Power Energy Eng. Conf. (APPEEC)*, Mar. 2009, pp. 1–4.
[9] M. A. Delucchi and T. E. Lipman, "Lifetime cost of battery, fuel-cell, and plug-in hybrid electric vehicles," in *Electric and Hybrid Vehicles: Power Sources, Models, Sustainability, Infrastructure and the Market*. Amsterdam, The Netherlands: Elsevier, 2010, pp. 19–60.
[10] S. Habib, M. M. Khan, F. Abbas, L. Sang, M. U. Shahid, and H. Tang, "A comprehensive study of implemented international standards, technical challenges, impacts and prospects for electric vehicles," *IEEE Access*, vol. 6, pp. 13866–13890, 2018.
[11] S. F. Tie and C. W. Tan, "A review of energy sources and energy management system in electric vehicles," *Renew. Sustain. Energy Rev.*, vol. 20, pp. 82–102, Apr. 2013.
[12] S. Kelouwani, K. Agbossou, Y. Dubé, and L. Boulon, "Fuel cell plug-in hybrid electric vehicle anticipatory and real-time blended-mode energy management for battery life preservation," *J. Power Sour.*, vol. 221, pp. 406–418, Jan. 2013.
[13] F. Odeim, J. Roes, and A. Heinzel, "Power management optimization of a fuel cell/battery/supercapacitor hybrid system for transit bus applications," *IEEE Trans. Veh. Technol.*, vol. 65, no. 7, pp. 5783–5788, Jul. 2016.
[14] J. Carroquino *et al.*, "Combined production of electricity and hydrogen from solar energy and its use in the wine sector," *Renew. Energy*, vol. 122, pp. 251–263, Jul. 2018.
[15] Goelectricity. (2017). *Datasheet Specs EPATH7500*. [Online]. Available: http://goelectricity.es/pdf/EPATH7500.pdf
[16] V. Roda, J. Carroquino, L. Valiño, A. Lozano, and F. Barreras, "Remodeling of a commercial plug-in battery electric vehicle to a hybrid configuration with a PEM fuel cell," *Int. J. Hydrogen Energy*, vol. 43, no. 35, pp. 16959–16970, 2018.
[17] O. Tremblay and L.-A. Dessaint, "Experimental validation of a battery dynamic model for EV applications," *World Elect. Veh. J.*, vol. 3, pp. 1–10, May 2009.
[18] J. M. Cabello, E. Bru, X. Roboam, F. Lacressonniere, and S. Junco, "Battery dynamic model improvement with parameters estimation and experimental validation," in *Proc. IMAACA*, Sep. 2015, pp. 63–70.
[19] C. Wang, B. Huang, and W. Xu, "An integrated energy management strategy with parameter match method for plug-in hybrid electric vehicles," *IEEE Access*, vol. 6, pp. 62204–62214, 2018.
[20] HDK. (2016). *Datasheet Sealed Lead-Acid HDFEV6A*. [Online]. Available: www.hdkev.com/docs/agm.pdf
[21] L. Serrao, Z. Chehab, Y. Guezennee, and G. Rizzoni, "An aging model of Ni-MH batteries for hybrid electric vehicles," in *Proc. IEEE Vehicle Power Propuls. Conf.* , Sep. 2005, p. 8.
[22] L. Serrao, S. Onori, G. Rizzoni, and Y. Guezennec, "A novel model-based algorithm for battery prognosis," *IFAC Proc. Volumes*, vol. 42, no. 8, pp. 923–928, 2009.
[23] V. Marano, S. Onori, Y. Guezennec, G. Rizzoni, and N. Madella, "Lithium-ion batteries life estimation for plug-in hybrid electric vehicles," in *Proc. IEEE Vehicle Power Propuls. Conf. (VPPC)*, Sep. 2009, pp. 536–543.
[24] A. Di Filippi, S. Stockar, S. Onori, M. Canova, and Y. Guezennec, "Model-based life estimation of Li-ion batteries in PHEVs using large scale vehicle simulations: An introductory study," in *Proc. IEEE Vehicle Power Propuls. Conf. (VPPC)*, Sep. 2010, pp. 1–6.
[25] L. Serrao, S. Onori, A. Sciarretta, Y. Guezennec, and G. Rizzoni, "Optimal energy management of hybrid electric vehicles including battery aging," in *Proc. Amer. Control Conf.*, Jun./Jul. 2011, pp. 2125–2130.
[26] M. Uzunoglu and M. S. Alam, "Modeling and analysis of an FC/UC hybrid vehicular power system using a novel-wavelet-based load sharing algorithm," *IEEE Trans. Energy Convers.*, vol. 23, no. 1, pp. 263–272, Mar. 2008.
[27] Z. Yu, D. Zinger, and A. Bose, "An innovative optimal power allocation strategy for fuel cell, battery and supercapacitor hybrid electric vehicle," *J. Power Sour.*, vol. 196, no. 4, pp. 2351–2359, 2011.
[28] V. Paladini, T. Donateo, A. de Risi, and D. Laforgia, "Super-capacitors fuel-cell hybrid electric vehicle optimization and control strategy development," *Energy Convers. Manage.*, vol. 48, no. 11, pp. 3001–3008, 2007.
[29] F. S. Alfonso *et al.*, "A study of hybrid powertrains and predictive algorithms applied to energy management in refuse-collecting vehicles," Ph.D. dissertation, Universitat Politècnica de Catalunya, Catalonia, Spain, 2015.
[30] L. Valverde, C. Bordons, and F. Rosa, "Integration of fuel cell technologies in renewable-energy-based microgrids optimizing operational costs and durability," *IEEE Trans. Ind. Electron.*, vol. 63, no. 1, pp. 167–177, Jan. 2016.
[31] J. S. Martinez, D. Hissel, M.-C. Pera, and M. Amiet, "Practical control structure and energy management of a testbed hybrid electric vehicle," *IEEE Trans. Veh. Technol.*, vol. 60, no. 9, pp. 4139–4152, Nov. 2011.
[32] S. N. Motapon, L.-A. Dessaint, and K. Al-Haddad, "A comparative study of energy management schemes for a fuel-cell hybrid emergency power system of more-electric aircraft," *IEEE Trans. Ind. Electron.*, vol. 61, no. 3, pp. 1320–1334, Mar. 2014.
[33] D. Feroldi and M. Carignano, "Sizing for fuel cell/supercapacitor hybrid vehicles based on stochastic driving cycles," *Appl. Energy*, vol. 183, pp. 645–658, Dec. 2016.
[34] C.-Y. Li and G.-P. Liu, "Optimal fuzzy power control and management of fuel cell/battery hybrid vehicles," *J. Power Sour.*, vol. 192, no. 2, pp. 525–533, 2009.
[35] P. García, J. P. Torreglosa, L. M. Fernández, and F. Jurado, "Control strategies for high-power electric vehicles powered by hydrogen fuel cell, battery and supercapacitor," *Expert Syst. Appl.*, vol. 40, no. 12, pp. 4791–4804, 2013.
[36] F. Barbir, *PEM Fuel Cells: Theory and Practice*. New York, NY, USA: Academic, 2012.
[37] L. Guzzella and A. Sciarretta, *Vehicle Propulsion Systems*, vol. 1. Berlin, Germany: Springer, 2007.
[38] A. Sciarretta, M. Back, and L. Guzzella, "Optimal control of parallel hybrid electric vehicles," *IEEE Trans. Control Syst. Technol.*, vol. 12, no. 3, pp. 352–363, May 2004.
[39] A. Sciarretta *et al.*, "A control benchmark on the energy management of a plug-in hybrid electric vehicle," *Control Eng. Pract.*, vol. 29, pp. 287–298, Aug. 2014.
[40] M. G. Carignano, R. Costa-Castelló, V. Roda, N. M. Nigro, S. Junco, and D. Feroldi, "Energy management strategy for fuel cell-supercapacitor hybrid vehicles based on prediction of energy demand," *J. Power Sour.*, vol. 360, pp. 419–433, Aug. 2017.
[41] D. E. Kirk, *Optimal Control Theory: An Introduction*. North Chelmsford, MA, USA: Courier Corporation, 2012.
[42] M. G. Carignano, N. Nigro, and S. Junco, "HEVs with reconfigurable architecture: A novel design and optimal energy management," in *Proc. Integr. Modeling Anal. Appl. Control Autom. (IMAACA)*, 2016, pp. 59–67.

MAURO CARIGNANO received the degree in mechanical engineering and the Ph.D. degree in engineering from the Facultad de Ciencias Exactas Ingenierí y Agrimensura, Universidad Nacional de Rosario (UNR), Rosario, Argentina, in 2011 and 2018, respectively. In 2016, he had a nine-month academic stage in Barcelona, Spain, focused on fuel cell-based propulsion system. Since 2012, he has been an Associate Professor of system dynamics and control with the Academic Staff, UNR. His research interests include optimal sizing of components and strategies of high-level supervisory control for hybrid electric vehicles.

VICENTE RODA received the degree in industrial technical engineering specializing in electricity from the University of Zaragoza (UZ), Spain, in 2008, the degree in hydrogen and fuel cell technologies from the CIRCE Foundation, UZ, in 2008, and the degree in microsystems and intelligent instrumentation from UZ, in 2009. His Diploma final project was developed with the research laboratory, Laboratorio de Investigación en Fluidodináąmica y Tecnologías de la Combustión (LIFTEC), Zaragoza. Between 2008 and 2012, he was with LIFTEC, where he was an In-charge of the Fuel Cell Laboratory, in which he focused on the development and assembly of test benches for fuel cells, and the development and assembly of fuel cells proton exchange membrane (PEM) type of high and low temperature. In 2012, he joined the Fuel Cell Control Group, Instituto de Robótica e Informática Industrial (IRI), Barcelona, where he was an In-charge of the improvement of the work stations, development of tests, and design of models based on the control of PEM fuel cells of both high and low temperature. From 2015 to 2016, he was hired by LIFTEC for the design and assembly of the hybridization of a battery-powered electric vehicle with a PEM fuel cell together with a solar energy system for the production of hydrogen, storage at 200 bar, and refueling of the vehicle for the European project LIFE13 ENV/ES/000280 LIFE + ReWIND. Since 2016, he has been responsible for the Fuel Cell Laboratory, IRI, where he is currently an In-charge of all test and test stations, participating in several projects at national and European levels.

RAMON COSTA-CASTELLÓ was born in Lleida, in 1970. He received the B.S. degree in computer science from the Universitat Politècnica de Catalunya (UPC), in 1993, and the Ph.D. degree in computer science from the Advanced Automation and Robotics Program, UPC, in 2001. He is currently an Associate Professor with the Automatic Control Department, UPC. His teaching activity is related to different aspects in automatic control. His research is mainly focused on analysis and development of energy management (automotive and stationary applications) and the development of digital control techniques. He is a member of the CEA and IFAC (EDCOM, TC 9.4 Committee, and Automotive Control T.C. 7.1) and a Senior Member of the IEEE.

LUIS VALIÑO was born in Madrid, in 1961. He received the degree and the Ph.D. degree in physics from the University of Zaragoza, in 1989, the degree from UNED, and the master's degree in economics from the University of Zaragoza. He holds a Postdoctoral position with Stanford University and NASA. He is currently a CSIC Scientific Researcher and the Director of the Laboratory of Research in Fluid Dynamics and Technologies of Combustion, a joint center between CSIC and the University of Zaragoza.

His research focused on stochastic methods applied to flows turbulent combustion problems (formation of pollutants) and dispersion of reactive pollutants in the atmosphere (ozone), and in the filtered two-phase flows (diesel injection). For a few years, he has been focusing on the modeling and simulation of polymer fuel cells. His research has focused on the transfer of knowledge to the industry. As a result, there are about 50 international publications, 60 projects and research contracts, and four patents.

ANTONIO LOZANO received the M.Sc. degree in physics from the University of Zaragoza, in 1984, and the Ph.D. degree in mechanical engineering from Stanford University, in 1992. He is currently a Scientific Researcher with the Laboratory for Research in Fluid Dynamics and Combustion Technology, a joint center between the Spanish National Research Council and the University of Zaragoza, Zaragoza, Spain. His areas of expertise are fuel cell design and applications, experimental fluid mechanics, and liquid atomization.

FÉLIX BARRERAS received the B.S. and M.S. degrees in mechanical engineering, with specialization in energy, from the University of Matanzas, Cuba, and the Ph.D. degree in industrial engineering (fluid mechanics) from the University of Zaragoza, Spain. He was a Professor with the Applied Physics Department, University of Matanzas, and for two other courses in the fluid mechanics area with the University of Zaragoza, for eight years. Since 2001, he has been a Senior Researcher with the Laboratory for Research in Fluid dynamics and Combustion Technologies, joint center of the Spanish National Research Council and the University of Zaragoza. He is also an Expert in the design of new nozzle for very heavy fuel oil or crude petroleum. Since 2002, he has been an In-charge of the fluid dynamics in polymer electrolyte membrane fuel cells (PEMFCs) research line. He focuses on the study of transport phenomena in PEMFCs, the optimal design of new flowfield for bipolar plates, and in the development of degradation tests for improving the durability and performance of these electrochemical devices. The sound experience acquired during these years has allowed to assemble prototypes up to 2 kW of electric power for different stationary and automotive applications. His research activities include the development and application of optical diagnostic technique to fluid mechanics, as planar laser-induced fluorescence and particle image velocimetry in both inert and combusting flows.